Fermi National Accelerator Laboratory

FERMILAB-Pub-75/80-THY
November 1975

Estimates of Charm Production in Exclusive Neutrino Reactions

R. E. Shrock and Benjamin W. Lee
Fermi National Accelerator Laboratory

ABSTRACT

We present calculations of the cross sections for two types of exclusive charm production reactions: the quasi-elastic processes $\nu N \to \mu^- (C_0, C_1, C_1^*)$ and the single pseudoscalar meson production processes $\nu N \to \mu^- K(C_0, C_1)$ and $\bar{\nu} N \to \mu^+ \bar{D}(\Lambda, \Sigma)$. With a set of reasonable assumptions we find that the ratio of the cross section for these exclusive channels to the inclusive non-charm cross section is $\sim 4\%$ for neutrinos and $\sim 3\%$ for antineutrinos.

Operated by Universities Research Association Inc. under contract with the Energy Research and Development Administration

I. INTRODUCTION

Recently there has been considerable interest, both theoretical and experimental, in the search for charmed particles.[1] The original motivation for the introduction of the fourth quark, c, carrying a new hadronic quantum number, charm, was the suppression of neutral strangeness-changing currents in gauge theories of weak interactions by means of the GIM mechanism.[2] Several experimental findings have provided support for the charm picture.[3] These include, first, the discovery of the narrow resonances $J/\psi(3.1)$ and $\psi'(3.7)$, for which the most plausible explanation seems to be that they are the ground state and a radial excitation, respectively, of a bound $c\bar{c}$ pair. Furthermore, the behavior of $R = \sigma(e^+e^- \to \text{hadrons})/\sigma(e^+e^- \to \mu^+\mu^-)$ clearly indicates the presence of more than just the three color triplets of u, d, and s quarks in hadrons. Thirdly, the Harvard-Penn-Wisconsin-FNAL experiment has observed an anomaly in the y distribution at small x and large y, in antineutrino deep inelastic scattering, such as would be caused by the production of a hadron with a new quantum number like charm. Both this group and the Caltach-FNAL group have observed dimuon events in neutrino and antineutrino reactions which again signal the production of hadrons with a new quantum number like charm. (The alternative explanation based on heavy lepton production is now reasonably well ruled out.) Finally, a $\Delta S = -\Delta Q$ event with the characteristic signature for charmed particle production and decay has been

observed in the Brookhaven bubble chamber experiment. Further and more decisive experimental verification of the existence of hadrons with charm (as well, probably, as other new quantum numbers) is presumably not too far in the future.

Theoretical estimates of cross sections and signatures for charm production have concentrated on deep inelastic neutrino reactions, including the contribution of F^* inelastic diffractive processes, and on e^+e^- annihilation.[4] Here we would like to consider the two simplest types of exclusive charm production reactions. These include, first, the quasi-elastic processes $\nu N \to \mu^- (C_0, C_1)$ and $\nu N \to \mu^- C_1^*$, where C_0 and C_1 are the $J^P = 1/2^+$, S = 0, C(charm) = 1, I = 0, 1 baryons, and C_1^* is the $J^P = 3/2^+$ analogue of C_1. (We follow the notation of Gaillard, Lee, and Rosner, Ref. 1.) The next simplest exclusive channels are the meson production reactions $\nu N \to \mu^- K(C_0, C_1)$ and $\bar{\nu} N \to \mu^+ \overline{D}\,(\Lambda, \Sigma)$, where D is the $J^P = 0^-$, S = 0, C = 1, I = 1/2 meson. The quasi-elastic reactions have lower thresholds than the meson production ones and consequently, other things being equal, would be a more favorable means of looking for charm. However, since the charm-changing part of the charged current in the GIM form of the Weinberg-Salam model is, in terms of quark fields,

$$J^{\mu}_{\Delta C} = \bar{c}\,\gamma^{\mu}(1 - \gamma_5)\left[-d\sin\theta_C + s\cos\theta_C\right] \qquad (1)$$

(where[5] $\theta_C = 0.239 \pm 0.005$ is the Cabibbo angle), and since the quasi-elastic channels necessarily involve the $d \to c$ transition, they are suppressed by the Cabibbo factor $\sin^2 \theta_C = 0.06$. In contrast, reactions in the subclass of the meson production processes which proceed via the $s \to c$ transition, namely the ones listed above, are proportional to $\cos^2 \theta_C$ and hence, despite their higher thresholds, are competitive with the quasi-elastic ones. These two types of exclusive reactions are of interest because they have the lowest thresholds of charm producing processes, and, for energies not too far above these thresholds, they are dominant among such processes. Accordingly, one can use them to obtain a rough estimate of charm production near threshold. A measure of this production rate is provided by the ratio of the cross section for the production of a final state containing charmed particles to the cross section for the production of an uncharmed final state:

$$R_N^{\nu, \bar{\nu}} = \frac{\sigma(\nu(\bar{\nu}) N \to \mu(\bar{\mu}) + \text{charm} + \ldots)}{\sigma(\nu(\bar{\nu}) N \to \mu(\bar{\mu}) + \ldots)} \quad . \tag{2}$$

Since these exclusive channels have cross sections which become constant as functions of incident neutrino energy E, they will be maximally visible under the linearly rising total inclusive (non-charm) cross section for energies not too far beyond their thresholds. As the energy increases, they will comprise a progressively smaller fraction of the total cross section. However, other higher multiplicity exclusive

channels yielding charmed particles will open and, presumably, $\sigma(\nu(\bar{\nu})N \to \mu(\bar{\mu}) + \text{charm} + \ldots)$ will scale at high energy, so that $R_N^{\nu,\bar{\nu}}$ will be approximately constant as a function of E.[6]

II. CALCULATIONS OF CROSS SECTIONS

Let us consider first the quasi-elastic reactions, which are, explicitly,

$$\nu n \to \mu^- C_0^+ \tag{3}$$

$$\nu p \to \mu^- C_1^{++} \tag{4}$$

$$\nu n \to \mu^- C_1^{+} \tag{5}$$

$$\nu p \to \mu^- C_1^{*++} \tag{6}$$

$$\nu n \to \mu^- C_1^{*+} \tag{7}$$

These are $\Delta Q = \Delta C = 1$, $\Delta S = 0$, $\Delta I = 1/2$ transitions. There are no antineutrino-induced quasi-elastic charm-producing reactions. Because of the $\Delta I = 1/2$ property of the current $J^{\mu}_{D^+}$ (i.e. the current having the same SU(4) transformation properties as the D^+ meson; the $\bar{c}\gamma^{\mu}(1 - \gamma_5)n$ current), the differential cross sections for reactions (4)-(7) satisfy the relations

$$\frac{d\sigma}{dQ^2}(\nu p \to \mu^- C_1^{++}) = 2\frac{d\sigma}{dQ^2}(\nu n \to \mu^- C_1^{+}) \tag{8}$$

$$\frac{d\sigma}{dQ^2}(\nu p \to \mu^- C_1^{*++}) = 2\frac{d\sigma}{dQ^2}(\nu n \to \mu^- C_1^{*+}) . \tag{9}$$

The invariant amplitudes for these reactions can be written in the form

$$\mathcal{M} = \frac{G \sin\theta_C}{\sqrt{2}} \bar{u}_\mu(\ell_2)\gamma_\lambda(1-\gamma_5)u_\nu(\ell_1)\left\langle C(p_2)\left| J^\lambda_{D^+}\right| N(p_1)\right\rangle \tag{10}$$

where $G = 1.02 \times 10^{-5}/m_N^2$. The matrix elements of the current $J^\mu_{D^+}$ can be calculated using SU(4) symmetry, as described in the Appendix. In terms of the usual F and D reduced matrix elements of the Cabibbo current between C = 0 SU(3) octet states we find

$$\left\langle C_0^+\left| J^\mu_{D^+}\right| n\right\rangle = \sqrt{\frac{3}{2}}\left(\frac{1}{3}D+F\right)^\mu \tag{11}$$

$$\left\langle C_1^{++}\left| J^\mu_{D^+}\right| p\right\rangle = \sqrt{\frac{3}{2}}\,(F-D)^\mu . \tag{12}$$

Since the vector part of the Cabibbo current is in the same SU(3) octet as the electromagnetic current, one can express the vector part of the F and D matrix elements in terms of matrix elements of the latter current. Writing

$$F^\mu = (F_V - F_A)^\mu \tag{13}$$

$$D^\mu = (D_V - D_A)^\mu \tag{14}$$

one obtains

$$F^\mu_V = \left\langle p\left| J^\mu_{em}\right| p\right\rangle + \frac{1}{2}\left\langle n\left| J^\mu_{em}\right| n\right\rangle \tag{15}$$

$$D^\mu_V = -\frac{3}{2}\left\langle n\left| J^\mu_{em}\right| n\right\rangle , \tag{16}$$

that is,

$$F_V^\mu = \bar{u}(p_2)\left[\left(F_1^p + \frac{1}{2}F_1^n\right)\gamma^\mu + \left(\mu_p F_2^p + \frac{1}{2}\mu_n F_2^n\right)\frac{i\sigma^{\mu\nu}q_\nu}{(m_N+m_C)}\right]u(p_1)\,, \qquad (17)$$

and similarly for D_V^μ. However, the vector part of J_D^μ is presumably dominated by the D^* meson, in contrast to the electromagnetic current, whose hadronic matrix elements exhibit vector meson dominance by ρ, ω, and ϕ. In order to take this into account we replace the vector dipole $(\text{mass})^2$, $0.71\ \text{GeV}^2$, in the Sachs form factor by $m_{D^*}^2$:

$$G_E^p(q^2) = \frac{G_M^p(q^2)}{1+\mu_p} = \frac{G_M^n(q^2)}{\mu_n} = \frac{1}{\left(1 - q^2/m_{D^*}^2\right)^2}\,, \qquad (18)$$

and $G_E^n(q^2) \simeq 0$. The Dirac and Pauli form factors are given by an obvious generalization of the usual relation to incorporate the mass difference between the initial and final baryons:

$$F_1^{p,n}(q^2) = \frac{\left(G_E^{p,n}(q^2) - \dfrac{q^2}{(m_N+m_C)^2}\,G_M^{p,n}(q^2)\right)}{\left(1 - \dfrac{q^2}{(m_N+m_C)^2}\right)} \qquad (19)$$

$$F_2^{p,n}(q^2) = \frac{\left(G_M^{p,n}(q^2) - G_E^{p,n}(q^2)\right)}{\left(1 - \dfrac{q^2}{(m_N+m_C)^2}\right)}\,. \qquad (20)$$

For the axial vector part of the F and D matrix elements we have:

$$(F_A^\mu,\ D_A^\mu) = \frac{(F,\ D)}{(F+D)} \left\langle p \left| \mathcal{F}_{1+i2}^{5\mu} \right| n \right\rangle , \tag{21}$$

where $\mathcal{F}_i^{5\mu}$ ($\mathcal{F}_i^{\mu}$) are the usual SU(3) octet axial-vector (vector) currents,

$$J_{\pi^+}^\mu = \mathcal{F}_{1+i2}^{\mu} - \mathcal{F}_{1+i2}^{5\mu} \tag{22}$$

$$\left\langle p \left| \mathcal{F}_{1+i2}^{5\mu} \right| n \right\rangle = (F+D)\, \bar{u}(p_2)\, \gamma^\mu \gamma_5\, F_A(q^2)\, u(p_1), \tag{23}$$

and[7]

$$\begin{aligned} F &= 0.78 \pm 0.02 \\ D &= 0.45 \pm 0.02 \end{aligned} \tag{24}$$

$$F_A(q^2) = \frac{1}{\left(1 - q^2/m_A^2\right)^2} . \tag{25}$$

In the actual matrix element of Eq. (21) the axial vector dipole mass is measured to be $m_A \simeq 0.95$ GeV.[8] However, for the matrix element of J_D^μ we shall use a value of m_A designed to reflect the dominance of the axial vector part of this current by charmed axial vector mesons. For definiteness we take m_A equal to the mass m_{D^*} used in the vector form factors. It should be noted, moreover, that in the expressions above we have assumed the absence of second class currents, so that there is no q^μ term in Eq. (17) and no $i\sigma^{\mu\nu} q_\nu \gamma_5$ term in Eq. (23).

Furthermore, we have neglected the induced pseudoscalar term $F_p(q^2)q^\mu\gamma_5$ since it gives a contribution proportional to muon mass.

Having determined the invariant amplitudes for the reactions (3) - (5), we next calculate the differential cross sections. For generality of notation, define

$$\left\langle C \left| J^\mu_{D+} \right| N \right\rangle = \bar{u}(p_2)\left[A(q^2)\gamma^\mu + B(q^2)\frac{i\sigma^{\mu\nu}q_\nu}{(m_N+m_C)} + C(q^2)\gamma^\mu\gamma_5\right]u(p_1), \quad (26)$$

where the form factors for the various reactions can be read off from Eqs. (11-16, 21-23). Then, neglecting muon mass (and using $Q^2 = -q^2$), we find

$$\frac{d\sigma}{dQ^2} = \frac{G^2\sin^2\theta_C}{8\pi E^2}\left[-2q^2W_1 + (4EE' + q^2)W_2 + \frac{\xi(E+E')}{m_N}q^2W_3\right], \quad (27)$$

where

$$W_1 = \frac{1}{4m_N^2}\left[\left\{(m_C - m_N)^2 - q^2\right\}|A+B|^2 + \left\{(m_C+m_N)^2 - q^2\right\}|C|^2\right] \quad (28)$$

$$W_2 = |A|^2 - \frac{q^2}{(m_N+m_C)^2}|B|^2 + |C|^2 \quad (29)$$

and

$$W_3 = 2\,\mathrm{Re}\left\{C^*(A+B)\right\} . \quad (30)$$

In Eq. (27) E' is the lab energy of the scattered muon and $\xi = \pm 1$ for $\nu, \bar{\nu}$ reactions, respectively. In connection with Eq. (30) one should

remark that the assumption of time reversal invariance implies that the form factors A, B, and C are real.

The analysis of the C_1^* reactions is more complicated and the results less reliable. We shall use two methods to estimate the cross sections for these reactions: first, a direct comparison with analogous processes involving uncharmed baryons, and, second, a calculation based on the isobar model. Proceeding with the first method, we record the SU(3) relation

$$\left\langle \Sigma^- \left| J^\mu_{K^-} \right| n \right\rangle = (D - F)^\mu \quad , \tag{31}$$

and the SU(4) result

$$\left\langle C_1^{*++} \left| J^\mu_{D^+} \right| p \right\rangle = \frac{2}{\sqrt{3}} \left\langle \Delta^{++}(1232) \left| J^\mu_{\pi^+} \right| p \right\rangle \quad , \tag{32}$$

where in the latter equation appropriate changes in the q^2 dependence of the form factors are understood. From Eqs. (12), (31), and (32) there then follows the approximate relation

$$\frac{\sigma(\nu p \to \mu^- C_1^{*++})}{\sigma(\nu p \to \mu^- \Delta^{++})} \simeq \frac{8}{9} \tan^2\theta_C \, \frac{\sigma(\nu p \to \mu^- C_1^{++})}{\sigma(\bar{\nu} n \to \mu^+ \Sigma^-)} \quad . \tag{33}$$

Although the hadronic matrix elements of J^μ_π and J^μ_D in the reactions $\bar{\nu} n \to \mu^+ \Sigma^-$ and $\nu p \to \mu^- C_1^{++}$ are proportional, in the cross sections the VA interference terms are of opposite sign. However, this is not an important effect since, as is evident from Eqs. (26) and (27), the VA term is

smaller than the dominant (VV, AA) term in the cross section by a full power of E, and consequently is negligible at high energies. It is, moreover, reasonable to assume that the enhancement of the charmed particle cross sections due to D^* (and the charmed axial-vector meson) dominance of the form factors is similar on both sides of Eq. (33). Then, using (1) the measured cross section[9] $\sigma(\nu p \to \mu^- \Delta^{++}) \simeq 0.7 \times 10^{-38} \text{cm}^2$, which is in accord with the prediction of the Adler theory[10] (for $m_A \simeq 0.95$ GeV); (2.) the Cabibbo prediction (again, for $m_A \simeq 0.95$ GeV) $\sigma(\bar{\nu} n \to \mu^+ \Sigma^-) \simeq 2 \times 10^{-40} \text{cm}^2$, and (3.) our result $\sigma(\nu p \to \mu^- C_1^{++}) \simeq 0.9 \times 10^{-39} \text{cm}^2$ for $m_{C_1} = 2.5$ GeV and $m_{D^*} = 2.26$ GeV, we get $\sigma(\nu p \to \mu^- C_1^{*++}) = 2\sigma(\nu n \to \mu^- C_1^{*+}) \simeq 1.6 \times 10^{-39} \text{cm}^2$.

In an effort to have a full dynamical calculation of the cross sections for the C_1^* reactions we have also utilized the isobar model, which treats the C_1^* as a stable particle. This model has been applied successfully to calculate weak production (as well as photo- and electroproduction) of the $\Delta(1232)$.[11] However, in the case of the C_1^* there is considerable uncertainty regarding the form factors which enter into the expression for the reaction amplitude. In addition, the isobar model suffers from a fundamental problem plaguing any calculation of a process involving particles of higher spin, namely that higher powers of momenta appear in the cross section and can give rise to spuriously large results at high energy. In particular, the spin projection operator which occurs when one performs the

summation over final baryon spin, contains terms going like the third power of the momentum.[12] The differential cross section still has the form

$$\frac{d\sigma}{dQ^2} \propto \frac{1}{E^2}\left[a_0 + a_1 E + a_2 E^2\right], \tag{34}$$

as a general result of the one intermediate vector boson exchange approximation,[13] but the dependence upon q^2 is increased by one power. If one did not include form factors to introduce damping in q^2 the cross section would grow without bound; even with form factors the higher powers of q^2 can give rise to spuriously large contributions at high energies. Where the model has been applied and compared with experimental data, such as in weak Δ production, the energy is sufficiently low so that this problem is not serious. In the present case we do not consider it justifiable to use the isobar model at energies more than 5-10 GeV above threshold.

With these caveats in mind, we continue with the calculation of the cross section for the C_1^* channels. The invariant matrix element can be written as a sum of four vector and axial vector terms. These will be specified by using Eq. (32) to relate them to the corresponding terms for Δ production. According to the usual convention the latter form factors are defined for the reaction $\nu n \to \mu^- \Delta^+$ Since J_π^μ is an isovector current, the form factors for the process $\nu p \to \mu^- \Delta^{++}$ are greater by $\sqrt{3}\ \langle \Delta^{++} | J^\mu_{\pi^+} | n \rangle$. Explicitly,

$$\mathcal{M}(\nu n \to \mu^- \Delta^+) = \frac{G}{\sqrt{2}} \bar{U}_\alpha(p_2) \left[\left(\frac{C_3^V}{m_N} \gamma_\beta + \frac{C_4^V}{m_N^2} p_{2\beta} + \frac{C_5^V}{m_N^2} p_{1\beta} \right) \gamma_5 F^{\beta\alpha} \right.$$

$$\left. + C_6^V j^\alpha \gamma_5 + \left(\frac{C_3^A}{m_N} \gamma_\beta + \frac{C_4^A}{m_N^2} p_{2\beta} \right) F^{\beta\alpha} + C_5^A j^\alpha + \frac{C_6^A \, q \cdot j \, p_1^\alpha}{m_N^2} \right] u(p_1), \quad (35)$$

where

$$j^\alpha = \bar{u}_n(\ell_2) \gamma^\alpha (1 - \gamma_5) u_\nu(\ell_1) \quad (36)$$

$$F^{\beta\alpha} = q^\beta j^\alpha - q^\alpha j^\beta, \quad (37)$$

and U_α is the Schwinger-Rarita spinor for the Δ. The fact that the vector current is conserved implies that $C_6^V = 0$ and the neglect of muon mass eliminates the C_6^A term. A detailed discussion of the remaining six form factors would be out of place here. We shall choose the q^2 dependence to be the same for all the nonzero form factors, viz.

$$C_i^{V,A}(q^2) \propto \frac{1}{\left(1 - q^2/m_{D^*}^2\right)^2} . \quad (38)$$

This ad hoc dipole parametrization is in reasonable agreement with the data on weak pion production. However, given the above-mentioned defect of the isobar model at high energies there is less justification for using dipole form factors in the C_1^* reactions. Accordingly, we have also tried phenomenological form factors having third order poles in (q^2/m_D^{*2}).

The $q^2 = 0$ values of the form factors used in successful models of Δ production, such as Adler's model, are listed below:[14]

$$C_3^V(0) \simeq 2.0$$

$$C_4^V(0) \simeq - \frac{m_N}{(m_N + m_\Delta)} \; C_3^V(0)$$

$$C_5^V(0) = 0$$

$$C_3^A(0) = 0 \qquad (39)$$

$$C_4^A(0) \simeq 0.3$$

$$C_5^A(0) = - 1.2$$

The value of $C_3^V(0)$ is well established from photo- and electroproduction data. This data can be fitted with C_4^V as given above, or with $C_4^V = 0$. The values of C_5^V, C_3^A, and C_5^A given in Eq. (39) are used in most models of Δ production. As for C_4^A, theories other than Adler's employ rather different values; for example, the static model has $C_4^A = 0$. The full expressions for the cross section is too long to include here; it is given, for example, by Albright and Liu, Ref. 11.

The final class of exclusive reactions to be considered consists of single pseudoscalar meson production processes. These include

reactions which proceed via both the $n \leftrightarrow c$ and the $s \leftrightarrow c$ transitions, but since we are interested only in the dominant channels we concentracte on the latter group of reactions. A list of them is given below:

$$\nu p \to \mu^- \left[K^+ C_0^+,\ K^+ C_1^+,\ K^0 C_1^{++} \right] \tag{40}$$

$$\nu n \to \mu^- \left[K^0 C_0^+,\ K^0 C_1^+,\ K^+ C_1^0 \right] \tag{41}$$

$$\bar{\nu} p \to \mu^+ \left[\bar{D}^0 \Lambda,\ \bar{D}^0 \Sigma^0,\ D^- \Sigma^+ \right] \tag{42}$$

$$\nu n \to \mu^+ \left[D^- \Lambda,\ D^- \Sigma^0,\ \bar{D}^0 \Sigma^- \right] \quad . \tag{43}$$

The reactions of Eqs. (40-41) and (42-43) are, respectively, $\Delta S = \Delta Q = \Delta C = \pm 1$, $\Delta I = 0$ transitions in which the hadronic weak current is $J^\mu_{F^\pm}$, the part of the charm-changing current transforming under SU(4) like the $F^\pm$ meson. As a consequence of the fact that J^μ_F is an isoscalar operator one immediately derives the following relations between the differential cross sections for these reactions:

$$\frac{d\sigma}{dQ^2}\left(\nu p \to \mu^- K^+ C_0^+\right) = \frac{d\sigma}{dQ^2}\left(\nu n \to \mu^- K^0 C_0^+\right) \tag{44}$$

$$\frac{d\sigma}{dQ^2}\left(\nu p \to \mu^- K^0 C_1^{++}\right) = \frac{d\sigma}{dQ^2}\left(\nu n \to \mu^- K^+ C_1^0\right)$$

$$= 2\,\frac{d\sigma}{dQ^2}\left(\nu p \to \mu^- K^+ C_1^+\right) = 2\,\frac{d\sigma}{dQ^2}\left(\nu n \to \mu^- K^0 C_1^+\right) \tag{45}$$

$$\frac{d\sigma}{dQ^2}\left(\bar{\nu}p \to \mu^+ \bar{D}^0 \Lambda\right) = \frac{d\sigma}{dQ^2}\left(\bar{\nu}n \to \mu^+ D^- \Lambda\right) \tag{46}$$

and finally,

$$\frac{d\sigma}{dQ^2}\left(\bar{\nu}p \to \mu^+ D^- \Sigma^+\right) = \frac{d\sigma}{dQ^2}\left(\bar{\nu}n \to \mu^+ \bar{D}^0 \Sigma^-\right)$$

$$= 2\,\frac{d\sigma}{dQ^2}\left(\bar{\nu}p \to \mu^+ \bar{D}^0 \Sigma^0\right) = 2\,\frac{d\sigma}{dQ^2}\left(\bar{\nu}n \to \mu^+ D^- \Sigma^0\right). \tag{47}$$

Note that, as was the case with the quasi-elastic reactions, charmed baryons are only produced by an incident neutrino beam, while antineutrinos yield only charmed mesons, with $C = -1$. In Figs. 1 and 2 are shown Born diagrams for illustrative reactions, in terms of quarks and physical particles. One may observe that there are no s-channel graphs since it is not possible for the favored $s \leftrightarrow c$ transition to take place off of the (valence) quarks of the target nucleon.

After these general remarks we shall briefly outline the calculation of the cross section for these meson production reactions. This is considerably more complicated than the case of quasi-elastic channels, as is indicated by the fact that the full differential cross section there is only a function of two variables, say E and q^2, whereas here it is a function of five variables. These can be conveniently chosen to be E, q^2, W (the invariant mass of the final meson-baryon system), and the polar and azimuthal (Treiman-Yang) angles

of emission of the meson in the hadron center of mass system, θ and ϕ.[15] In order to determine the amplitude we shall use the method of the generalized Born approximation, in which one includes only diagrams without loops but utilizes phenomenological form factors for the weak vertices. This approximation is based on the assumption that the Born poles in the s, u, and t channels provide the main contribution to the amplitude, simply because they are the nearest singularities to the physical region. It is also supported by phase space arguments which show that single particle intermediate states should dominate over multiparticle intermediate states at low energies. The Born approximation by itself, of course, does not take into account resonances. It is thus presumably most reliable near threshold in nonresonant reactions. At higher energies the model breaks down, because (1) most of the physical region is farther and farther from the Born poles, so that the assumption of Born pole dominance is no longer valid, and (2) the nonrenormalizable Pauli magnetic moment coupling terms contribute spuriously large terms to the amplitude.[16] Moreover, the Born model yields a cross section which grows linearly with energy at sufficiently high energy, in conflict with the observed behavior of cross sections for exclusive processes (which, as was mentioned before, reach constant values or decrease at high energies). This spurious growth arises from the integral over W, the upper limit of which increases with E. Accordingly, one must cut off this integral, at some upper

limit W_{max}. In a resonant process such as weak pion production a natural cutoff is provided by the width of the Δ resonance; i.e. $W_{max} \simeq W_{res} + \Gamma$.[17] In contrast, there is no natural cutoff in the reactions considered here, and thus we shall show results based on several different choices of W_{max}.

Turning, then, to the calculation of the Born amplitude, we note that, as is clear from Figs. 1 and 2, the $KC_{0,1}$ reactions receive contributions from Λ and Σ exchange in the u channel, respectively, and from $\bar{D}$ exchange in the t channel, while the $\bar{D}(\Lambda, \Sigma)$ reactions involve C_0 and C_1 exchange in the u channel, respectively, and K exchange in the t channel. In the spirit of the simple Born approximation we do not include the contributions due to the Y^* resonances in the u channel or K^*, D^*, and other meson resonances in the t channel. In order to calculate the matrix elements of the weak hadronic current J^μ_F we shall make use of SU(4) symmetry. In particular, in the case of the baryon matrix elements we shall again use the symmetry between transitions in the octet comprised of the particles N, C_1, C_0, and X and transitions in the regular $C = 0$ baryon octet. In terms of the F and D reduced matrix elements we find

$$\left\langle C_0^+ \left| J^\mu_{F^+} \right| \Lambda \right\rangle = \frac{1}{3} D^\mu + F^\mu \tag{48}$$

$$\left\langle C_1 \left| J^\mu_{F^+} \right| \Sigma \right\rangle = F^\mu - D^\mu . \tag{49}$$

In this case, in order to incorporate F^* dominance of the vector part of J^μ_F and the analogous charmed axial vector meson dominance of the axial vector part of this current, we use m_{F^*} in place of m_{D^*} in the modified form factors dealt with above. Similarly, for the matrix elements of the current between meson states (in which only the vector part contributes)

$$\begin{aligned}\left\langle K(k_2)\left|J^\mu_{F^{++}}\right|\bar{D}(k_1)\right\rangle &= \left\langle K^0(k_2)\left|J^\mu_{K^+}\right|\pi^-(k_1)\right\rangle \\ &= f_+(q^2)(k_1+k_2)^\mu + f_-(q^2)(k_1-k_2)^\mu ,\end{aligned} \tag{50}$$

where $f_+(q^2)$ and $f_-(q^2)$ are the form factors for $K_{\ell 3}$ decay and $J^\mu_{K^+} = \mathscr{J}^\mu_{4+i5} - \mathscr{J}^{5\mu}_{4+i5}$. The f_- term contributes a term proportional to lepton mass and is dropped. We take $f_+(q^2)$ to have a dipole form, with the mass parameter equal to m_{F^*}.

One must next determine the coupling constants to use for the strong Yukawa vertices in the Born graphs. One obtains the following relevant SU(4) symmetric coupling terms in the effective strong interaction Lagrangian (with γ_5 suppressed):

$$\begin{aligned} i\mathscr{L} &= g_{NDC_0}\left[\bar{C}_0^+ p D^0 + \bar{C}_0^+ n D^+\right] + \\ &+ g_{NDC_1}\left[\overline{C_1^+}\left(p D^0 - n D^+\right) + \sqrt{2}\left(\overline{C_1^0}\, n D^0 + \overline{C_1^{++}}\, p D^+\right)\right] + \text{h.c.}\end{aligned} \tag{51}$$

These terms are the same as the $NK\Lambda$ and $NK\Sigma$ interaction terms, with the replacements $\bar{D}^0 \leftrightarrow K^+$, $D^- \leftrightarrow K^0$, $C_0^+ \leftrightarrow \Lambda$, $C_1^{0,+,++} \leftrightarrow \Sigma^{-,0,+}$

and $g_{NDC_0} \leftrightarrow g_{NK\Lambda}$, $g_{NDC_1} \leftrightarrow g_{NK\Sigma}$. SU(4) symmetry, or actually just the symmetry between the MBB couplings of the octet containing N, C_1, C_0, and X, and the usual $C = 0$ octet implies that

$$g_{NDC_0} = g_{NK\Lambda}$$
$$g_{NDC_1} = g_{NK\Sigma} \quad , \tag{52}$$

where the latter coupling constants are defined as

$$g_{NK\Lambda} = \frac{-(3-2\alpha)}{\sqrt{3}} \, g_{\pi NN}$$
$$g_{NK\Sigma} = (2\alpha - 1) \, g_{\pi NN} \tag{53}$$

with $g_{\pi NN} \simeq 13.5$ and $\alpha = D/(F+D)$ the coefficient of the symmetric MBB coupling. For $\alpha \simeq 0.6$ (corresponding to the SU(6) prediction $F/D = 2/3$), we have

$$g_{NK\Lambda} \simeq -14$$
$$g_{NK\Sigma} \simeq 2.7 \tag{54}$$

Experimentally, these coupling constants have not been measured very precisely.[18] Although the measurements are scattered over rather large ranges, they indicate that central values of $g_{NK\Lambda}$ and $g_{NK\Sigma}$ fall somewhat below the SU(3) predictions. For example,

$(g_{NK\Lambda})_{exp.} \simeq -10$. However, there is no unambiguous way to incorporate SU(3) symmetry breaking in the formulas (48, 49), which are based on the assumption of SU(4) symmetry. Consequently, we shall use the SU(3) symmetric values listed in Eq. (54).

The determination of the weak W boson-hadron couplings, as given by the matrix elements of the current J_F between the relevant baryon or meson states, and the specification of the Yukawa couplings, suffice to evaluate the amplitude for the pseudoscalar meson production reactions in Born approximation. It is then straightforward, although rather tedious, to calculate the differential cross section, which is

$$\frac{\partial^4 \sigma}{\partial Q^2 \partial W^2 \partial \cos\theta \, \partial\phi} = \frac{1}{2^7 m_N^2 E^2 (2\pi)^4} \frac{|\vec{p}_2|}{W} |\mathcal{M}|^2 , \qquad (55)$$

where $\mathcal{M}$ is the invariant amplitude, and $\vec{p}_2$ is the 3-momentum of the final baryon in the hadron center of mass frame. In order to obtain the cross section we then integrate over the four variables ϕ, θ, W, and Q^2. To facilitate the integration over the azimuthal angle ϕ it is useful to decompose the differential cross section into the five terms allowed by the Pais-Treiman theorem, which have the explicit ϕ dependence: 1, $\cos\phi$, $\sin\phi$, $\cos 2\phi$, and $\sin 2\phi$, respectively.[13] The integration over ϕ leaves a three-fold integral which is evaluated numerically on a computer.

III. NUMERICAL RESULTS

Because our primary goal is the estimate of charm production we shall not present the differential cross sections, but rather only the total cross sections. The results are dependent, of course, on the values which one takes for the charmed particle masses. Estimates of these masses have been given by a number of authors, in particular, Gaillard, Lee, and Rosner,[1] and de Rujula, Georgi, and Glashow.[19] For reference it will be useful to list their results for the relevant masses; these are shown in Table I. It might be noted that we have updated the GLR estimate of m_D by using $m_{\eta_c} \simeq 2.8$ GeV.[20] An experimental measure of the charmed baryon mass scale is provided by the Brookhaven $\Delta S = -\Delta Q$ event, with $m_C \simeq 2.4$ GeV. The masses have two major effects on the behavior of the cross section. First, obviously, the threshold in incident neutrino energy depends quadratically on the invariant mass of the final hadronic state and increases rapidly as the charmed particle masses are increased. Second, the masses which enter into the dipole form factors, which we have chosen to be m_{D^*} and m_{F^*} for the reactions involving J_D^μ and J_F^μ, respectively, control the Q^2 behavior of the differential cross section $d\sigma/dQ^2$. As one increases these mass parameters $d\sigma/dQ^2$ is less rapidly damped in Q^2 and the total cross section increases commensurately. In order to show this dependence on the dipole mass parameter, in

Fig. 3 we exhibit the cross section $\sigma(\nu n \to \mu^- C_0^+)$ with $m_{C_0} = 2.5$ GeV, for several different values of m_{D^*} from 1.9 GeV to 2.5 GeV. Evidently, the cross section increases by about a factor of two as m_{D^*} is varied through this range.

In Figs. 4 and 5 we present $\sigma(E)$ for the reaction $\nu n \to \mu^- C_0^+$, for $m_{D^*} = 1.95$ and 2.26 GeV, respectively, and for m_{C_0} in the range from 2.0 to 4.0 GeV. As expected, the cross sections rise from threshold and, for $E \gtrsim E_{th} + 10\,\text{GeV}$ become roughly constant. Note that the levelling off takes longer the larger the dipole mass is. Next, in Figs. 6 and 7 are shown the cross sections for the dominant C_1 reaction, $\nu p \to \mu^- C_1^{++}$ with the same variation of the masses m_{D^*} and m_{C_0}. These are somewhat smaller than the corresponding cross sections for $\nu n \to \mu^- C_0^+$; for example, at $E = 10$ GeV, for $m_{D^*} = 2.26$ GeV and $m_{C_0} = m_{C_1} = 2.5$ GeV,

$$\frac{\sigma(\nu p \to \mu^- C_1^{++})}{\sigma(\nu n \to \mu^- C_0^+)} = \frac{2\sigma(\nu n \to \mu^- C_1^+)}{\sigma(\nu n \to \mu^- C_0^+)} \simeq 0.4 \quad . \tag{56}$$

In Fig. 8 we plot the cross sections for the dominant C_1^* reaction $\nu p \to \mu^- C_1^{*++}$ as calculated in the isobar model, with $m_{D^*} = 1.95$ GeV and $m_{C_1^*}$ in the range from 2.0 to 4.0 GeV. Curves (8a-c) represent the dipole parametrization given in Eq. (38); for comparison curves (8d-f) show the results of using form factors with a third order pole in q^2. Each plot is cut off 10 GeV above threshold. We consider these

cross sections to be spuriously large but include them for completeness to illustrate the results of the isobar model calculation.

Let us next discuss the meson production cross sections which are not suppressed by a small Cabibbo factor. First, in order to illustrate the dependence of these cross sections on the cutoff used in the integral over W, we show in Fig. 9 the cross section for one of these reactions, $\nu p \to \mu^- K^+ C_0^+$, for several values of $\Delta W = W_{max} - W_{th}$. For these curves we have taken $m_{C_0} = 2.5$ GeV, $m_{F^*} = 2.2$ GeV, and $m_D = 2.0$ GeV. A reasonable physical criterion on which to base the choice of ΔW is the requirement that the cross section level off for energies not too far above E_{th}, in units of W_{th}, say. Admittedly somewhat arbitrarily, we have chosen $\Delta W = 0.3$ GeV for the graphs of the meson production reactions to be shown below; from Fig. 9 the reader can infer how the cross sections would change as a function of ΔW if one were to choose a different value of this cutoff.

The cross sections for the two types of neutrino reactions $\nu N \to \mu^- K C_0$ and $\nu N \to \mu^- K C_1$ are presented in Figs. 10 and 11. Specifically, the curves shown are $\sigma(\nu p \to \mu^- K^+ C_0^+)$ and $\sigma(\nu p \to \mu^- K^0 C_1^{++})$; the others in Eqs. (40-41) can be determined from the relations given in Eqs. (42-43). For these calculations we have taken the mass parameter used in the vector and axial vector form factors equal to $m_{F^*} = 2.2$ GeV, $m_D = 2.0$ GeV, and have varied m_{C_0} and m_{C_1} over the range from 2.0 to

4.0 GeV . Evidently, $\sigma(\nu p \to \mu^- K^+ C_0^+) \gg \sigma(\nu p \to \mu^- K^0 C_1^{++})$, which is primarily a consequence of the fact that the former cross section is proportional to $g_{NK\Lambda}\, g_{NDC_0} = g_{NK\Lambda}^2$, while the latter is proportional to $g_{NK\Sigma}\, g_{NDC_1} = g_{NK\Sigma}^2$, and $g^2_{NK\Lambda}/g^2_{NK\Sigma} = 27$ (for the choices of Eq. (54)). Finally, Figs. 12 and 13 show the cross sections for the other two types of meson production reactions, i.e., the ones leading to charmed mesons (with C = -1) rather than charmed baryons: $\bar{\nu}N \to \mu^+ \bar{D}\Lambda$ and $\bar{\nu}N \to \mu^+ \bar{D}\Sigma$. For these curves we take the same value of m_{F^*} as above, and $m_{C_0} = m_{C_1} = 2.5$ GeV, and vary m_D over the range from 1.8 GeV to 2.6 GeV. The specific cross sections shown are $\sigma(\bar{\nu}p \to \mu^+ \overline{D^0} \Lambda)$ and $\sigma(\nu p \to \mu^+ D^- \Sigma^+)$; the others can again be obtained from Eq. (43-44). One observes again that the channel with an I = 0 baryon, in this case $\bar{\nu}p \to \mu^+ \overline{D^0} \Lambda$, is dominant over that with an I = 1 baryon, $\bar{\nu}p \to \mu^+ D^- \Sigma^+$, and the reason is the same as the one mentioned before. In general, even the dominant meson production reactions are somewhat smaller than the quasi-elastic ones.

From these cross section computations we can next determine the ratios of charm production via these channels to the total inclusive non-charm cross section for ν and $\bar{\nu}$ reactions. These ratios, based on the simplest exclusive channels, are of interest because it is these channels which can be most easily identified with 3C fits in bubble chambers. At higher energy in higher multiplicity channels, there

are more neutral particles (eg. π^0's, K^0's) and it is commensurately more difficult to identify events positively as $\Delta S = -\Delta Q$ or find enhancements in invariant mass distributions. We shall use the well-established experimental results [21]

$$\sigma(\nu N \to \mu^- X) = (0.78 \times 10^{-38}\ \text{cm}^2/\text{GeV})E \tag{57}$$

$$\sigma(\bar{\nu} N \to \mu^+ X) = (0.28 \times 10^{-38}\ \text{cm}^2/\text{GeV})E$$

$$\simeq \frac{1}{3}\sigma(\nu N \to \mu^- X) \tag{58}$$

for ν and $\bar{\nu}$ reactions in an average nucleon. For the separate proton and neutron cross sections, we use the recent measurement [22]

$$\frac{\sigma^{\nu n}}{\sigma^{\nu p}} \simeq 1.5$$

and assume that $\frac{\sigma^{\bar{\nu} n}}{\sigma^{\bar{\nu} p}} \simeq 1.5$ also. The ratios will be calculated at E = 10 GeV ; presumably at this energy the channels included in our analysis comprise the main part of charm production. In Tables IIA, B and III are listed the cross sections for the various channels contributing to $\sigma(\nu p \to \mu^- + \text{charm})$, $\sigma(\nu n \to \mu^- + \text{charm})$ and the corresponding $\bar{\nu}$ reactions. For the quasi-elastic charmed baryon reactions, we take $m_{D^*} = 2.26$ GeV and $m_{C_{0,1}} \simeq m_{C_1^*} \simeq 2.5$ GeV, while for the meson production processes, we assume the same C_0 and C_1 masses, $m_{F^*} = 2.2$ GeV, $m_D = 2.0$ GeV, and $\Delta W = 0.3$ GeV. Finally, in the case of the C_1^* reactions we take the estimate based on Eq. (33). From these results one then calculates $R_N^\nu \simeq R_p^\nu \simeq R_n^\nu \simeq 4\%$,

and $R_N^{\bar{\nu}} \simeq R_p^{\bar{\nu}} \simeq R_n^{\bar{\nu}} \simeq 3\%$. If one wishes to assume different values for certain charmed particle masses, he can use the various cross section curves to recalculate these ratios. Qualitatively they will increase for larger values of m_{D^*} and m_{F^*} and decrease for larger values of m_D, $m_{C_{1,0}}$ and $m_{C_1^*}$. It is not so easy to estimate the effects of SU(4) symmetry breaking on the cross section calculations and we have not pursued this question in detail.

Let us next apply our ratios for charm production in neutrino reactions to the Brookhaven bubble chamber experiment. The data in this experiment consist of 62K pictures of reactions in hydrogen and 220K in deuterium. In accordance with the Brookhaven estimates,[3] we assume that the branching ratio of charmed hadrons into experimentally identifiable strange particles is $\sim$ 50% and the ratio of charm events with and without neutrals is similar to that observed at similar energies in associated strange particle production, namely 50%. Using these numbers, together with the quoted number [74] of events with E > 4 GeV, we arrive at a rough estimate of the number of charm production events which should have been identified in the Brookhaven experiment: 0.8 events.

Finally, it should be noted that the quasi-elastic reactions $\nu N \to \mu^- C_{0,1}$ and $\nu N \to \mu^- C_1^*$ have also been studied by Finjord and Ravndal,[23] using a relativistic quark model. However, they fail to take into account the fact that the charm-changing weak hadronic current

J_D^μ is dominated by the D^*; instead, they use form factors having mass parameters like those of the electromagnetic current. Consequently, they obtain cross sections considerably smaller than those calculated above.

ACKNOWLEDGEMENT

We would like to thank C. Albright and S. Treiman for several valuable conversations. We would also like to thank our experimental colleagues, especially D. Cundy, F. DiBianca, F. Nezrick, W. Palmer and N. Samios for stimulating our interest in this problem.

APPENDIX

We shall briefly illustrate here the calculation of the matrix elements of the weak charm current. For $N \to C_1$ transitions, we have (suppressing Lorentz indices)

$$\langle C_1 | J_{D^+} | N \rangle = \langle 1 I_3 | \tfrac{1}{2}\tfrac{1}{2}\tfrac{1}{2} \pm \tfrac{1}{2} \rangle \begin{pmatrix} 6 & 3 & 8 \\ C_1 & \bar{D} & N \end{pmatrix} \sum_\gamma \begin{pmatrix} 20 & 15 & 20\gamma \\ 6 & 3 & 8 \end{pmatrix} \langle 20 \| 15 \| 20\gamma \rangle \tag{A1}$$

which yields

$$\langle C_1^{++} | J_{D^+} | p \rangle = 2 \langle C_1^{+} | J_{D^+} | n \rangle$$

$$= \frac{-17}{4\sqrt{78}} \langle 20 \| 15 \| 20_1 \rangle - \sqrt{\frac{2}{13}} \langle 20 \| 15 \| 20_2 \rangle \tag{A2}$$

Similarly, for $n \to C_0$

$$\langle C_0^{+} | J_{D^+} | n \rangle = \begin{pmatrix} 3^* & 3 & 8 \\ C_0 & \bar{D} & N \end{pmatrix} \sum_\gamma \begin{pmatrix} 20 & 15 & 20\gamma \\ 3^* & 3 & 8 \end{pmatrix} \langle 20 \| 15 \| 20\gamma \rangle$$

$$= \frac{3\sqrt{3}}{4\sqrt{26}} \langle 20 \| 15 \| 20_1 \rangle - \sqrt{\frac{2}{13}} \langle 20 \| 15 \| 20_2 \rangle \ . \tag{A3}$$

The two reduced matrix elements in these expressions are present because the $\underline{20}$ representation of SU(4) containing the $J^P = \frac{1}{2}^+$ baryons occurs twice in the decomposition of $\underline{15} \times \underline{20}$ into irreducible representations, as shown in Fig. 14.

In terms of the usual F and D reduced matrix elements,

$$\langle 20 \| 15 \| 20_1 \rangle = \frac{8}{\sqrt{13}} D$$

$$\langle 20 \| 15 \| 20_2 \rangle = \frac{5\sqrt{3}}{6\sqrt{13}} D - \frac{\sqrt{39}}{2} F \qquad \text{(A4)}$$

From Eqs. (A1) - (A4) one obtains the results given in Eqs. (11-12). The matrix elements of the weak current J_F are determined in the same way as those of J_D .

FOOTNOTES AND REFERENCES

[1] M. K. Gaillard, B. W. Lee, and J. L. Rosner, Rev. Mod. Phys. 47, 277 (1975); A. de Rujula, H. Georgi, and S. Glashow, Rev. Mod. Phys. 46, 391 (1974); B. W. Lee, in the Proceedings of the International Symposium on Lepton and Photon Interactions, Stanford University, 1975, and references therein.

[2] S. Glashow, J. Iliopoulos, and L. Mainani, Phys. Rev. D2, 1285 (1970).

[3] For discussions of the present status of e^+e^- annihilation experiments and the new particles, see the talks of G. Abrams, G. Feldman, F. Gilman, H. Harari, M. Perl, R. Schwitters, and B. Wiik in the Proceedings of the International Symposium on Lepton and Photon Interactions, Stanford University, 1975. The results of the Harvard-Pennsylvania-Wisconsin-FNAL, Caltech-FNAL, Brookhaven, and Gargamelle neutrino experiments are discussed respectively by C. Rubbia, B. Barish, N. Samios, and D. Perkins at the SLAC Symposium, op. cit. On the HPWF experiment, see also D. Cline, in the Proceedings of the International Conference on High Energy Physics, Palermo, Sicily.

[4] See, for example, the works of Ref. 1, and: C. H. Albright, Nucl. Phys. B75, 539 (1974); G. Altarelli et al., Phys. Lett. 48B, 435 (1974); M. Einhorn and C. Quigg, "Nonleptonic Decays of Charmed Mesons: Implications for e^+e^- Annihilation," FERMILAB-Pub-75/21-THY; ibid., Phys. Rev. Lett. 35, 1114 (1975);

M. Einhorn and B. W. Lee, "Contribution of Vector Meson Dominance to Charmed Meson Production in Inelastic Neutrino and Antineutrino Interaction," FERMILAB-Pub-75/56-THY; B. W. Lee, in Proceedings of the International Symposium on Lepton and Photon Interactions, Stanford University, ibid., in the Proceedings of the Conference on Gauge Theories and Modern Field Theory, Northeastern University; M. K. Gaillard, S. Jackson, and D. Nanopoulos, "Diffractive Elastic Neutrino Production of Vector Mesons," CERN preprint TH. 2049; V. Barger and T. Weiler "Vector Meson Dominance Calculations for the $\bar{\nu}$ Anomaly and Dimuon Production," Wisconsin preprint C00-456; V. Barger, T. Weiler, and R. Phillips, Phys. Rev. Lett. 35, 692 (1975), ibid. "Right-Handed Currents in Neutrino Scattering," Wisconsin preprint C00-466, among other references.

[5]The value of θ_C is from the one-angle fit in L.-M. Chounet, J.-M. Gaillard and M. K. Gaillard, Phys. Repts. 4C, 199 (1972).

[6]Indeed the Harvard-Pennsylvania-Wisconsin-FNAL dimuon data indicate that this ratio is roughly equal at 50 and 100 GeV; cf. C. Rubbia, in Ref. 3, A. Benvenuti, et al., Phys. Rev. Lett. 35, 1199 (1975).

[7]The F and D values are from Chounet, Gaillard and Gaillard, Ref. 5.

[8]P. Schreiner, in Neutrinos 1974; Proceedings of the Fourth International Conference on Neutrino Physics and Astrophysics, Philadelphia (AIP, 1974).

[9]J. Campbell, et al., Phys. Rev. Lett. 30, 335 (1973); P. Schreiner and F. von Hippel, Phys. Rev. Lett. 30, 339 (1973); P. Schreiner, Ref. 8.

[10] S. Adler, Annals of Physics (New York), 50, 189 (1968).

[11] Isobar model calculations include: M. Gourdin and P. Salin, Nuovo Cimento 27, 193, 309 (1963); C. Albright and L. Liu, Phys. Rev. Lett. 13, 673 (1964); Phys. Rev. 140B , 748, 1611 (1965); S. Berman and M. Veltman, Nuovo Cimento 38, 993 (1965); C. Kim, Nuovo Cimento 37, 142 (1965); P. Salin, Nuovo Cimento 48A, 506 (1967), A. Dufner and Y. Tsai, Phys. Rev. 168, 1801 (1968); J. Bijtebier, Nucl. Phys. B21, 158 (1970). Two recent reviews, the notation of which we shall follows, are C. Llewellyn-Smith, Phys. Repts. 3C, 261 (1972) and P.Schreiner, op. cit., Ref. 8.

[12] Explicitly,

$$\sum_{r=-3/2}^{3/2} U_\mu^{(r)}(p)\overline{U}_\nu^{(r)}(p) = \left(\frac{\not{p}+m}{2m}\right)\left[g_{\mu\nu} - \frac{1}{3}\gamma_\mu\gamma_\nu - \frac{2p_\mu p_\nu}{3m^2} + \frac{p_\mu\gamma_\nu - p_\nu\gamma_\mu}{3m}\right].$$

[13] The one intermediate vector boson exchange approximation is equivalent to locality in the limit of large m_W. See T. D. Lee and C. N. Yang, Phys. Rev. 126, 2239 (1962), A. Pais and S. Treiman, in "Problems of Theoretical Physics," an Anniversary Volume Dedicated to N. N. Bogoliubov (Moscow, Nauka, 1969), p. 279; Phys. Rev. D1, 907 (1970).

[14] Adler's model (Ref. 10) is of course a full dispersion theoretic analysis of pion production, not just an isobar model; the $q^2 = 0$ values of the

of the form factors listed in Eq. (39) represent the translation of the resultant amplitude in terms of the isobar model (Bijtebier, Ref. 11). A comparison of the predictions of various models with experimental data is given by P. Schreiner, and F. von Hippel, op. cit., Ref. 9, and P. Schreiner, Ref. 8.

[15] For a discussion of the kinematics of these reactions, see S. Adler, Ref. 10 and R. Shrock, Phys. Rev. D12, to be published.

[16] There are other problems in using the Born approximation at higher energies. For example, the inclusion of both s and t channel exchanges is in contradiction with duality.

[17] Indeed, in the spirit of resonance dominance by the $\Delta(1232)$, Adler cuts off the W integrals at $W_{max} = 1.39$ or 1.47 GeV.

[18] For a compilation of relevant experimental data, see H. Pilkuhn, et al., Nucl. Phys. B65, 460 (1973).

[19] A. de Rujula, H. Georgi, and S. Glashow, Phys. Rev. D17, 147 (1975).

[20] B. Wiik, Ref. 3.

[21] See eg., D. Cundy, in Proceedings of the International Conference on High Energy Physics, London, 1974, and Ref. 3.

[22] N. Samios, Ref. 3. See also Cazzoli, et al., and M. Hagenauer, in La Physique du Neutrino à Haute Energie , (Paris, 1975). For reference, the valence quark model prediction is

$$\frac{\sigma^{\nu n}}{\sigma^{\nu p}} = \frac{\sigma^{\bar{\nu} p}}{\sigma^{\bar{\nu} n}} = 2 \ ;$$

the sea contribution reduces this number.

[23] J. Finjord and F. Ravndal, Phys. Lett. 58B, 61 (1975).

TABLE AND FIGURE CAPTIONS

Table I — Estimates of relevant charmed hadron masses [sources: Gaillard, Lee and Rosner (GLR), Ref. 1 and de Rujula, Georgi, and Glashow (RGG), Ref. 19] . Units: GeV; notation (m_1 , m_2) means $m_1 \lesssim m \lesssim m_2$.

Table II — Cross sections for exclusive charm producing neutrino reactions at E = 10 GeV

(A) proton target

(B) neutron target

See text for values of masses.

Table III — Cross sections for charm producing antineutrino reactions at E = 10 GeV, on protons. See text for values of masses. The entries for the corresponding reactions on neutrons are the same.

FIGURES

Fig. 1 — Generic Born diagrams for the reactions $\nu N \to \mu^- KC_{0,1}$ (a) with elementary fields, (b) with physical hadrons.

Fig. 2 — Generic Born diagrams for the reactions $\bar{\nu}N \to \mu^+ \bar{D}Y$ ($Y = \Lambda_1 \Sigma$) (a) with elementary fields, (b) with physical hadrons.

Fig. 3 $\sigma(E)$ for the reaction $\nu n \to \mu^- C_0^+$, with m_{C_0} = 2.5 GeV and m_{D^*} = (a) 1.9, (b) 2.1, (c) 2.3, (d) 2.5 GeV.

Fig. 4 $\sigma(E)$ for the reaction $\nu n \to \mu^- C_0^+$ with m_{D^*} = 1.95 GeV and m_{C_0} = (a) 2.0, (b) 3.0, (c) 4.0 GeV.

Fig. 5 $\sigma(E)$, as in Fig. (4) but with m_{D^*} = 2.26 GeV.

Fig. 6 $\sigma(E)$ for the reaction $\nu p \to \mu^- C_1^{++}$ with m_{D^*} = 1.95 GeV and m_{C_1} = (a) 2.0, (b) 3.0, (c) 4.0 GeV.

Fig. 7 $\sigma(E)$, as in Fig. (6), but with m_{D^*} = 2.26 GeV.

Fig. 8 $\sigma(E)$ for the reaction $\nu p \to \mu^- C_1^{*++}$ as calculated in the isobar model with m_{D^*} = 1.95 GeV. Curves (a), (b), and (c) are calculated for dipole form factors and $m_{C_1^*}$ = 2.0, 3.0, and 4.0 GeV, respectively, while curves (d), (e), and (f) are calculated with form factors having third order poles and $m_{C_1^*}$ = 2.0, 3.0, and 4.0 GeV, respectively.

Fig. 9 $\sigma(E)$ for the reaction $\nu p \to \mu^- K^+ C_0^+$, with m_{F^*} = 2.2 GeV, m_{C_0} = 2.5 GeV, m_D = 2.0 GeV, and ΔW = (a) 0.1, (b) 0.2, (c) 0.3, (d) 0.4 GeV.

Fig. 10 $\sigma(E)$ for the reaction $\nu p \to \mu^- K^+ C_0^+$, with m_{F^*} = 2.2 GeV, m_D = 2.0 GeV and m_{C_0} = (a) 2.0, (b) 3.0, (c) 4.0 GeV.

Fig. 11 $\sigma(E)$ for the reaction $\nu p \to \mu^- K^0 C_1^{++}$, with m_{F^*} and m_D as in Fig. 10, and m_{C_1} = (a) 2.0, (b) 3.0, (c) 4.0 GeV.

Fig. 12 $\sigma(E)$ for the reaction $\bar{\nu}p \to \mu^+ \overline{D^0} \Lambda$, with $m_{F^*} = 2.2$ GeV, $m_{C_0} = 2.5$ and $m_D =$ (a) 1.8 (b) 2.2 (c) 2.6 GeV.

Fig. 13 $\sigma(E)$ for the reaction $\bar{\nu}p \to \mu^+ D^- \Sigma^+$ with the same masses as in Fig. 12.

Fig. 14 Clebsch-Gordan decomposition of $\underline{20} \times \underline{15}$ in SU(4).

Particle	GLR	RGG
C_0	(2.7, 6)	(2.20, 2.30)
C_1	(2.6, 4.4)	(2.36, 2.46)
C_1^*	(2.7, 4.2)	(2.42, 2.52)
D'	2.0	(1.80, 1.86)
D^*	2.26	(1.93, 1.99)
F^*	2.31	2.06

TABLE I

(A)

REACTION	$\sigma(E=10\ GeV), 10^{-39} cm^2$
$\nu p \rightarrow \mu^- C_1^{++}$	0.9
$\nu p \rightarrow \mu^- C_1^{*++}$	1.6
$\nu p \rightarrow \mu^- K^+ C_0^+$	0.4
$\nu p \rightarrow \mu^- K^+ C_1^+$ + $\nu p \rightarrow \mu^- K^0 C_1^{++}$	0.03
$\nu p \rightarrow \mu^-$ + charm	2.9

(B)

REACTION	$\sigma(E=10\ GeV), 10^{-39} cm^2$
$\nu n \rightarrow \mu^- C_0^+$	2.3
$\nu n \rightarrow \mu^- C_1^+$	0.5
$\nu n \rightarrow \mu^- C_1^{*+}$	0.8
$\nu n \rightarrow \mu^- K^0 C_0^+$	0.4
$\nu n \rightarrow \mu^- K^+ C_1^0$ + $\nu n \rightarrow \mu^- K^0 C_1^+$	0.03
$\nu n \rightarrow \mu^-$ + charm	4.0

TABLE 2

REACTION	σ(E=10 GeV), 10^{-39}cm^2
$\bar{\nu}p \rightarrow \mu^+ \bar{D}^0 \Lambda$	0.8
$\bar{\nu}p \rightarrow \mu^+ \bar{D}^0 \Sigma^0$ + $\bar{\nu}p \rightarrow \mu^+ D^- \Sigma^+$	0.06
$\bar{\nu}p \rightarrow \mu^+$ + charm	0.9

TABLE 3

(1a)

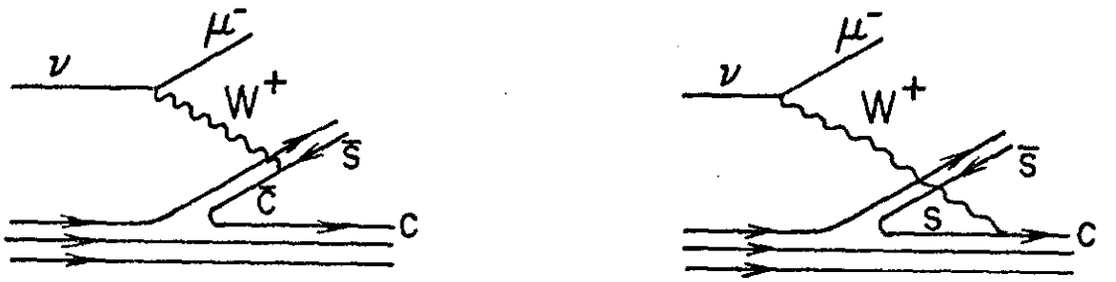

(1b)

Fig. 1

(2a)

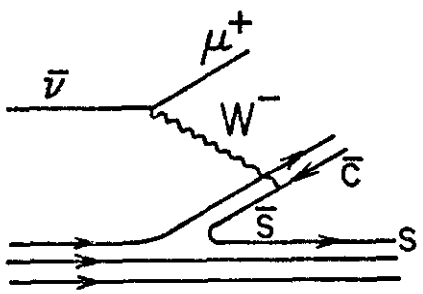
$\bar{\nu}$
μ^+
W^-
$\bar{c}$
$\bar{s}$
s

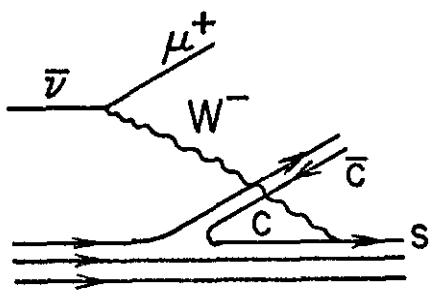
$\bar{\nu}$
μ^+
W^-
$\bar{c}$
c
s

(2b)

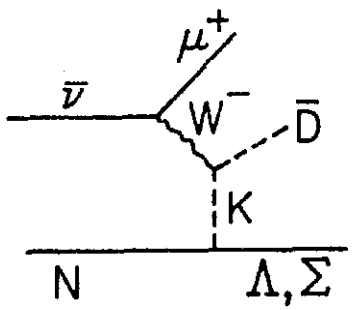
$\bar{\nu}$
μ^+
W^-
$\bar{D}$
K
N
Λ, Σ

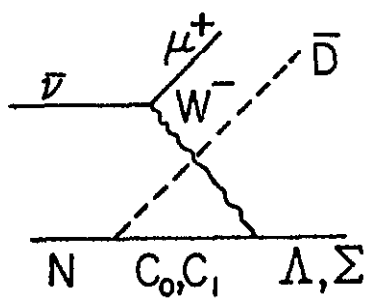
$\bar{\nu}$
μ^+
W^-
$\bar{D}$
N
C_0, C_1
Λ, Σ

Fig. 2

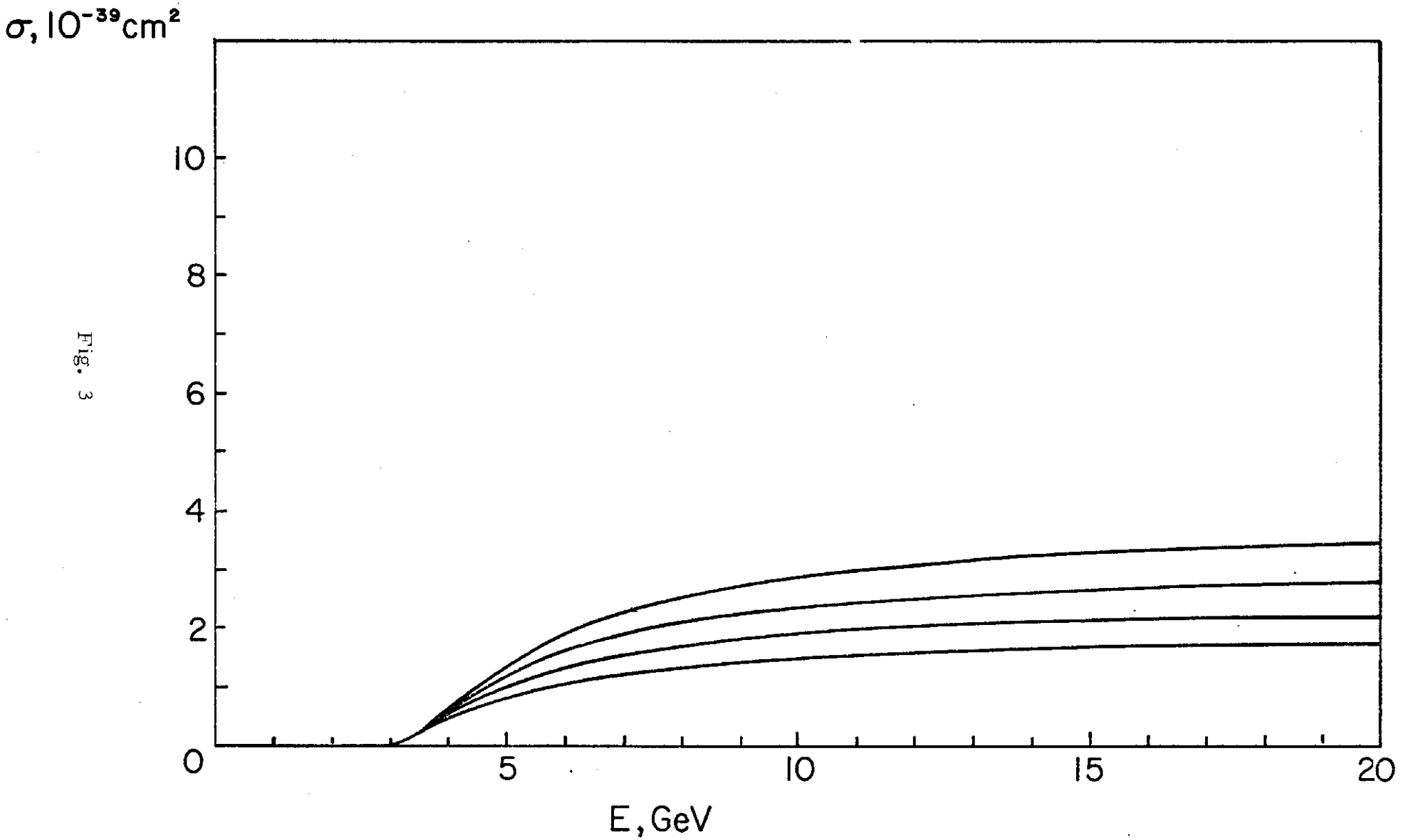

Fig. 3

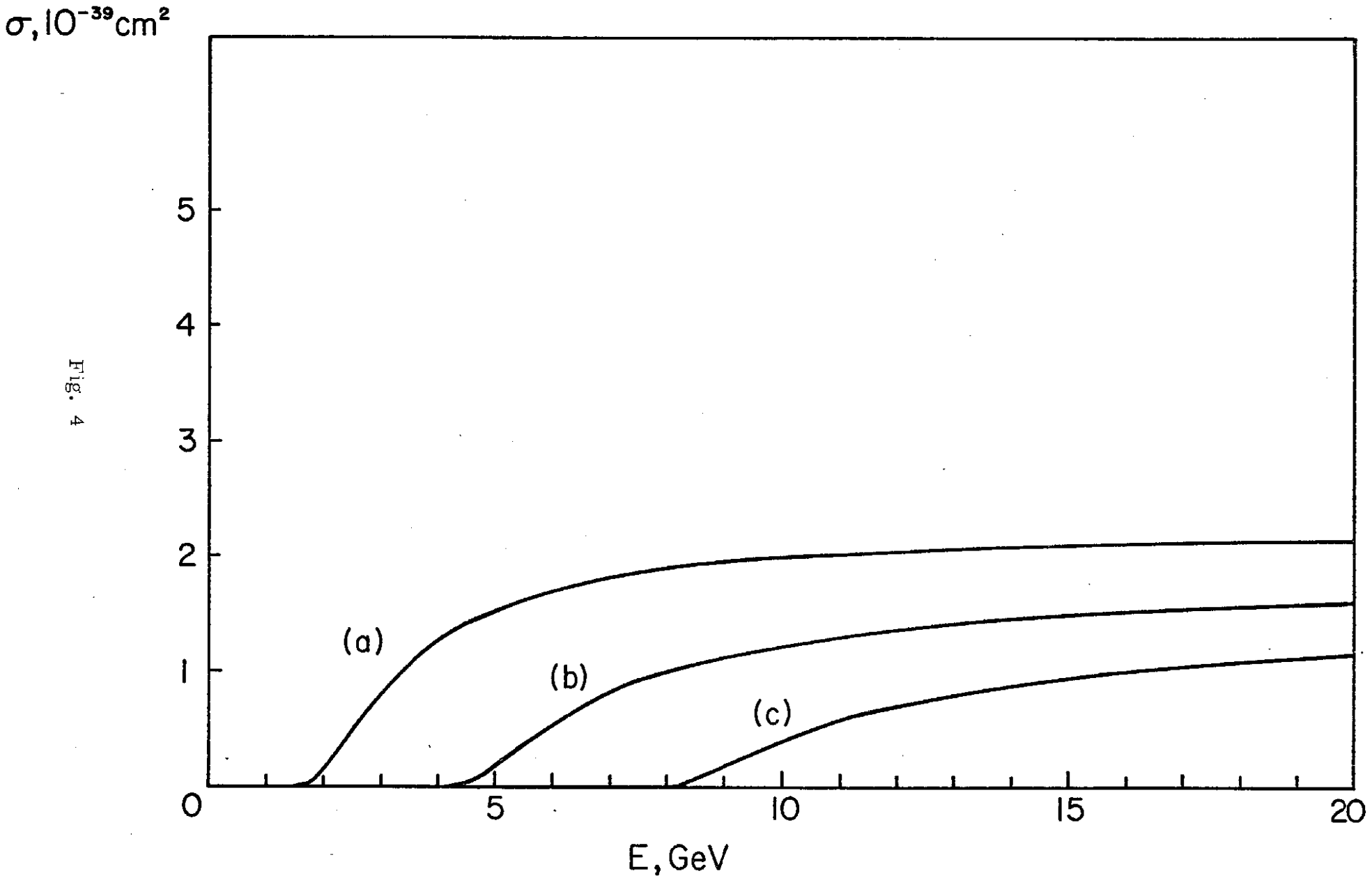

Fig. 4

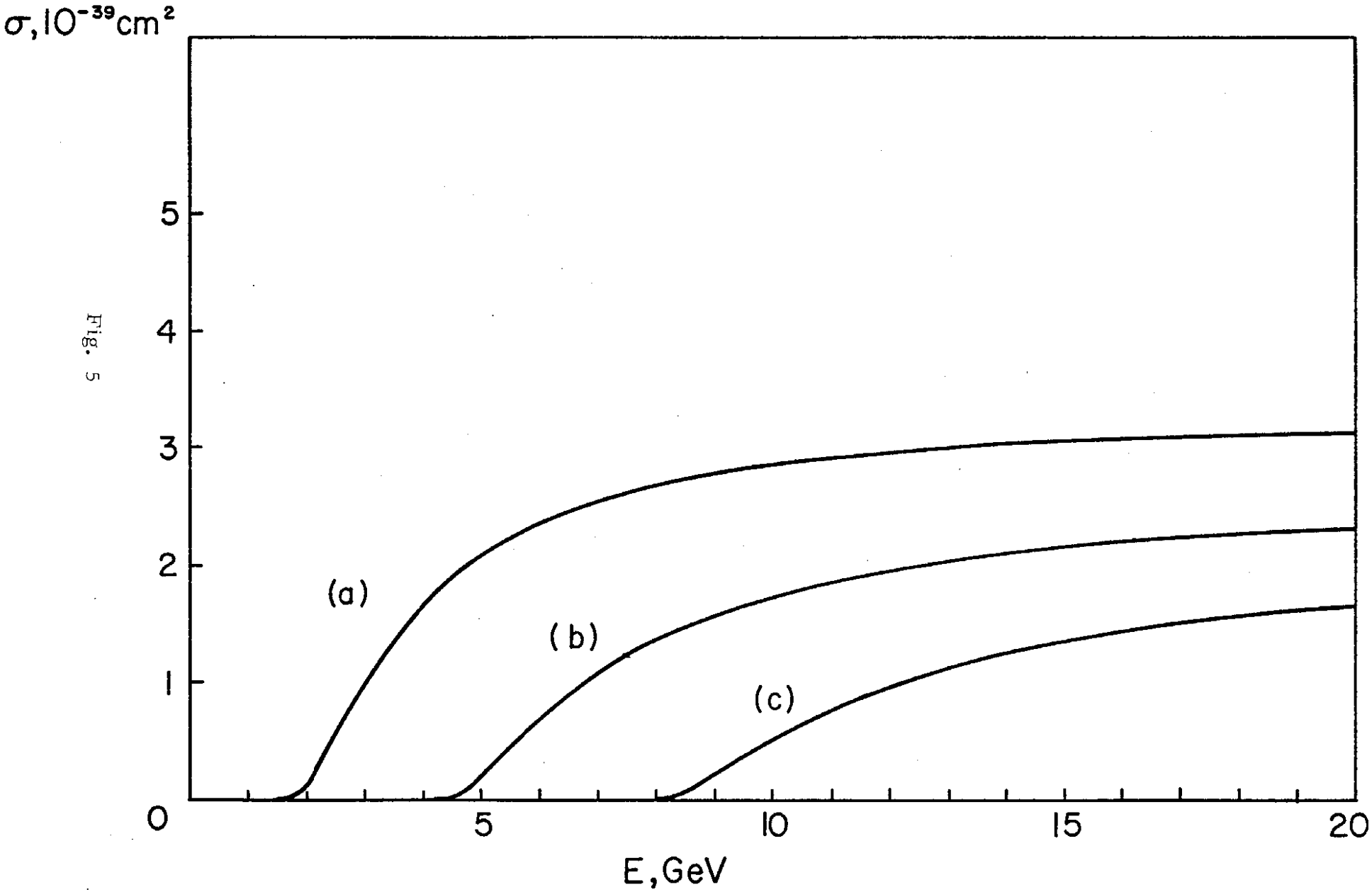

Fig. 5

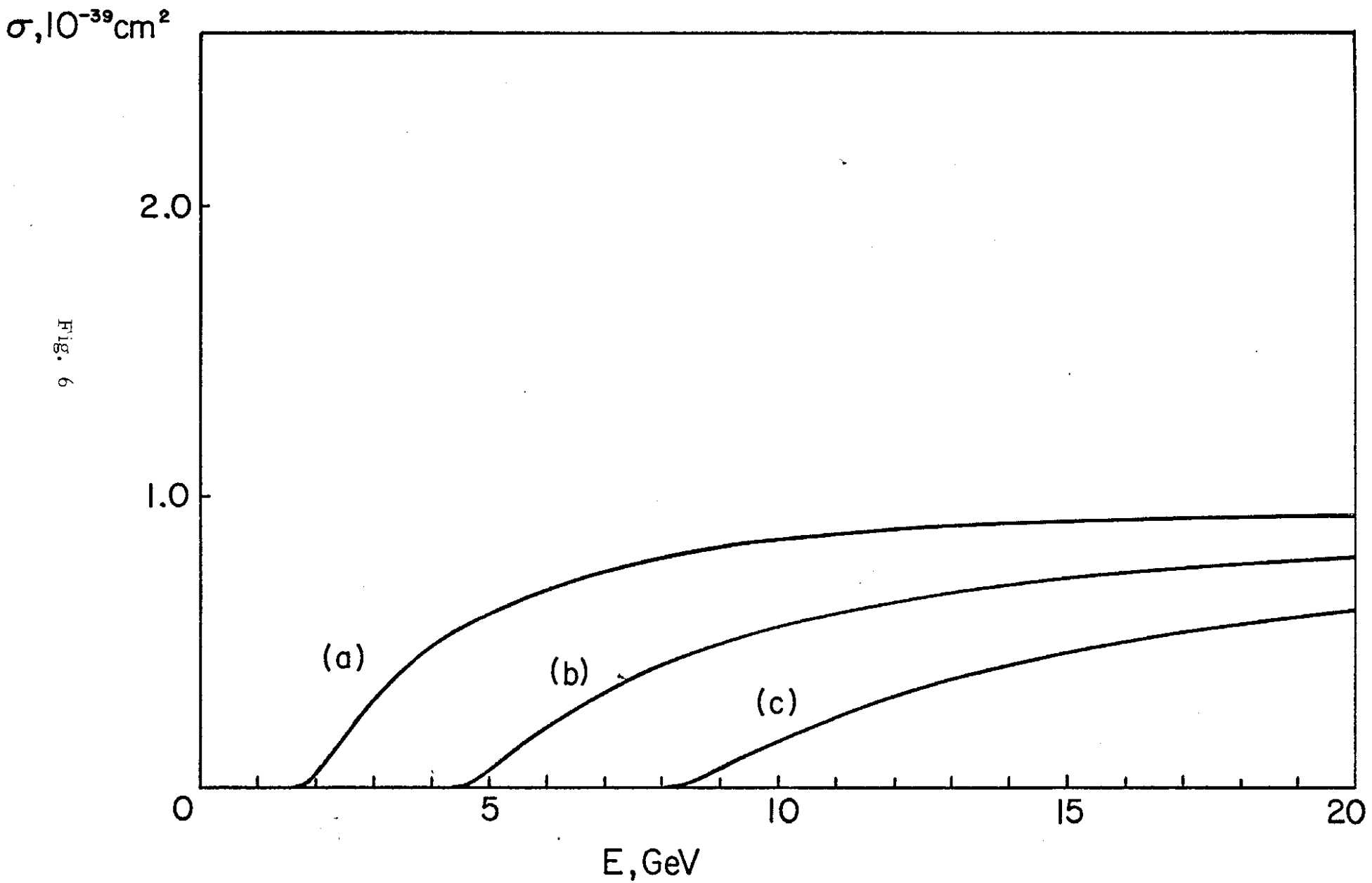

Fig. 6

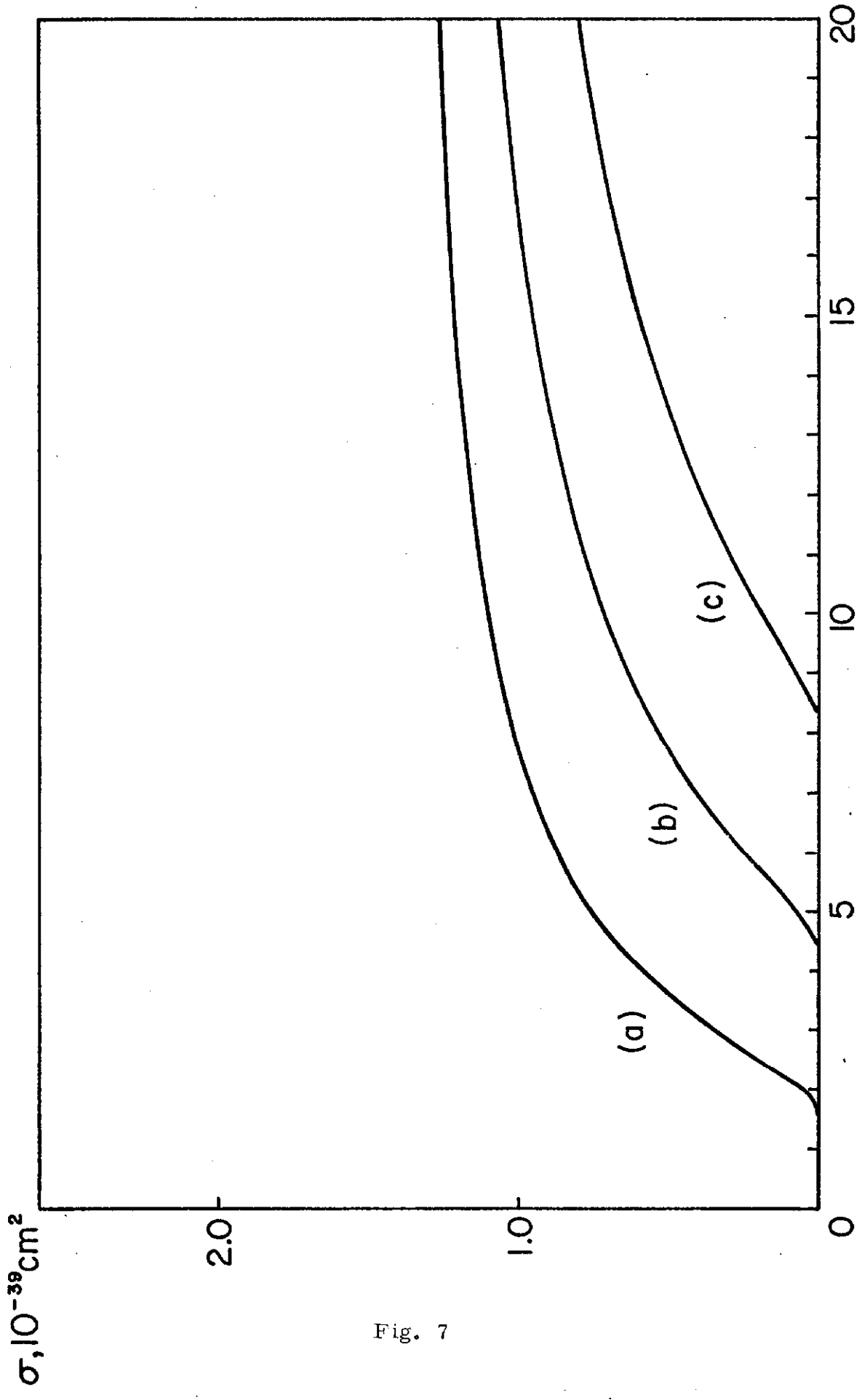

Fig. 7

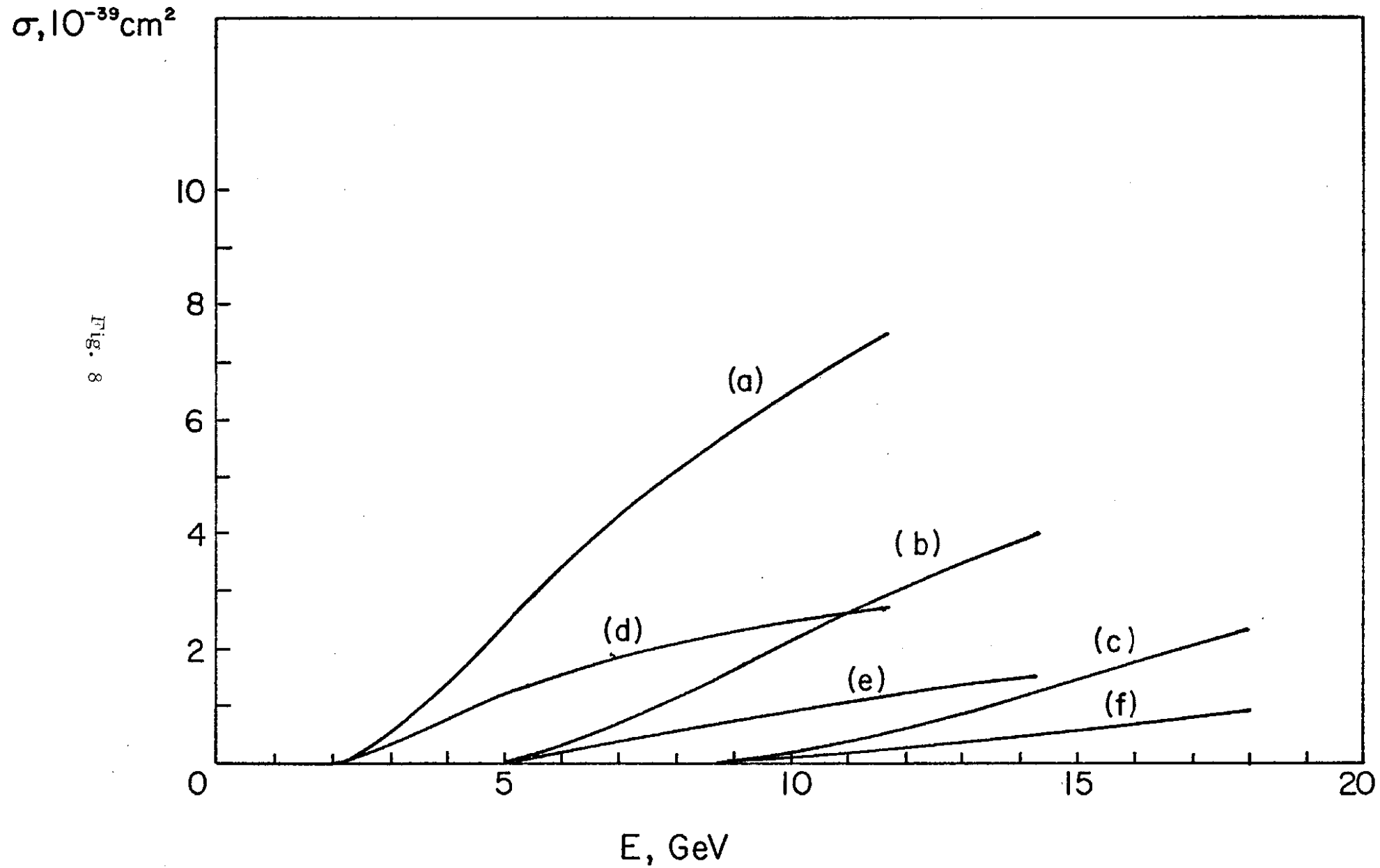

Fig. 8

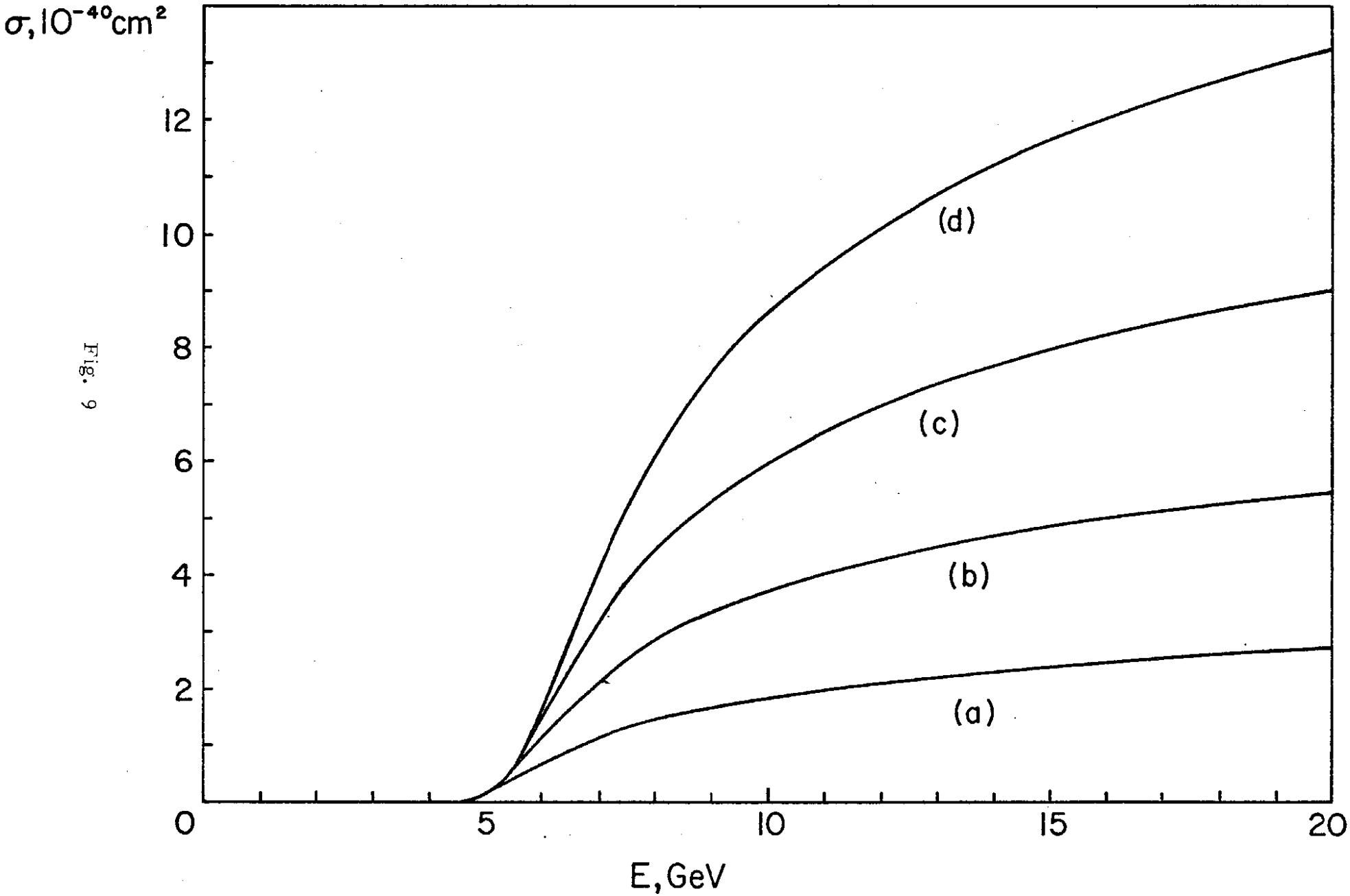

Fig. 9

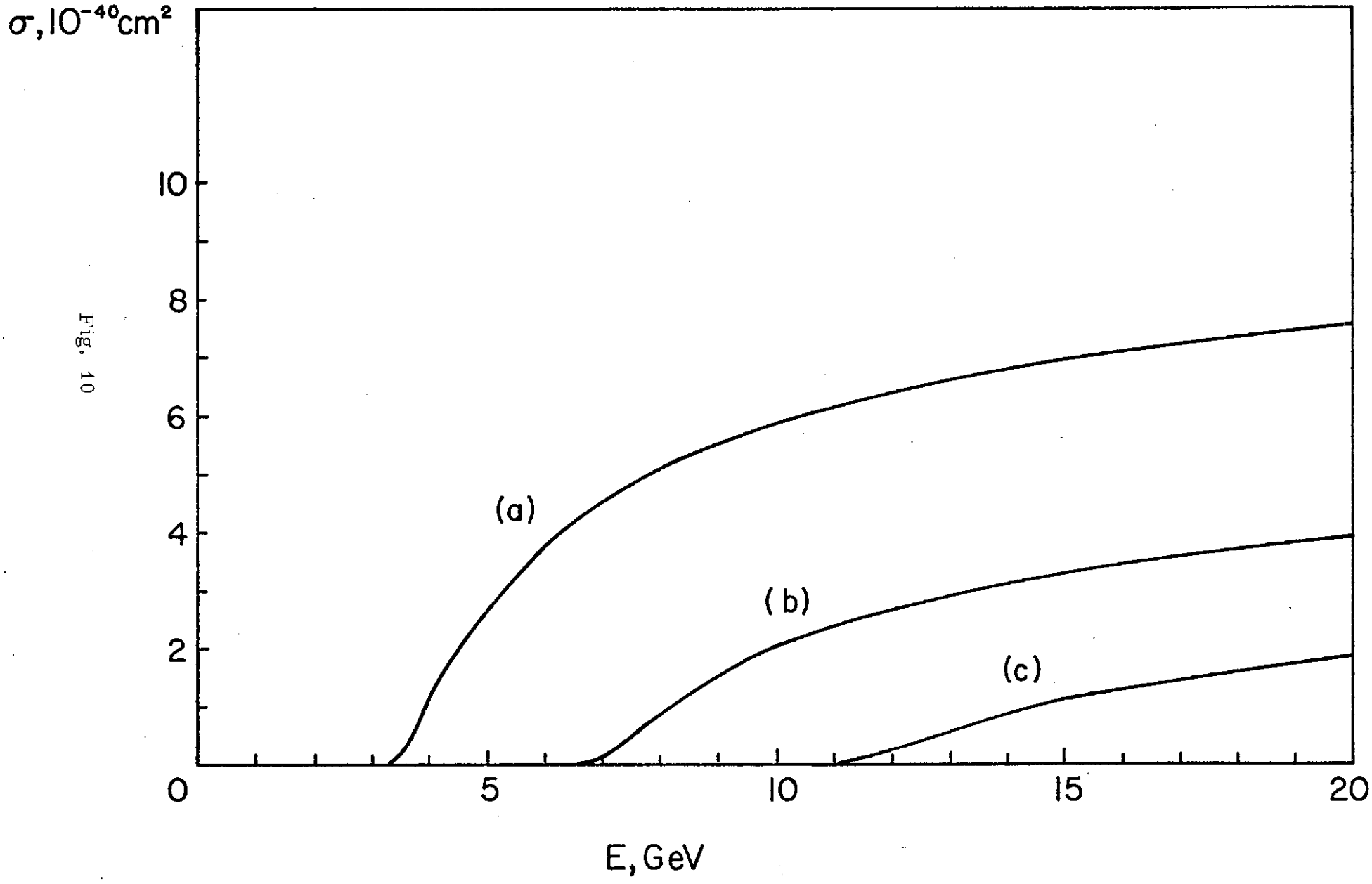

Fig. 10

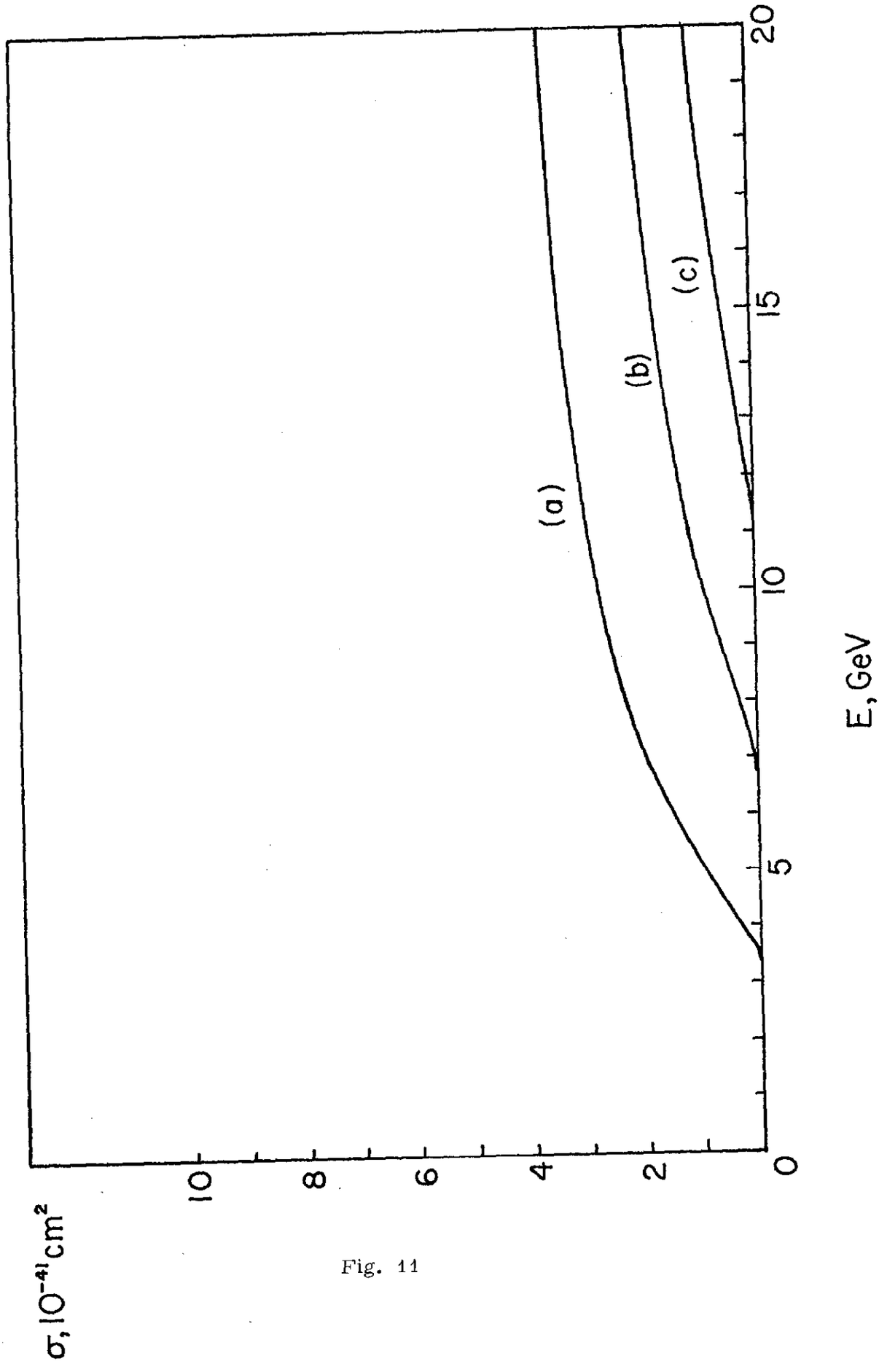

Fig. 11

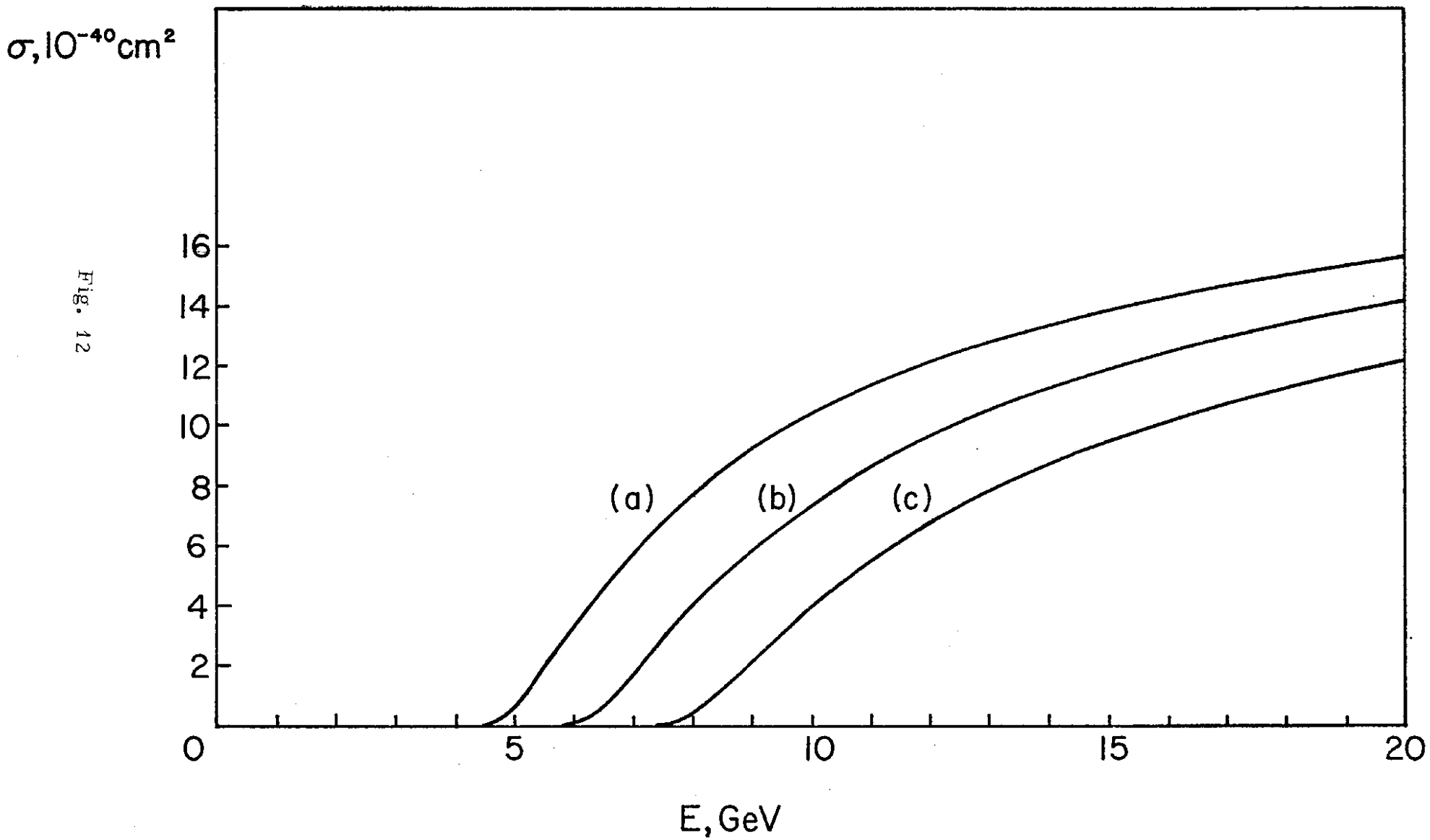

Fig. 12

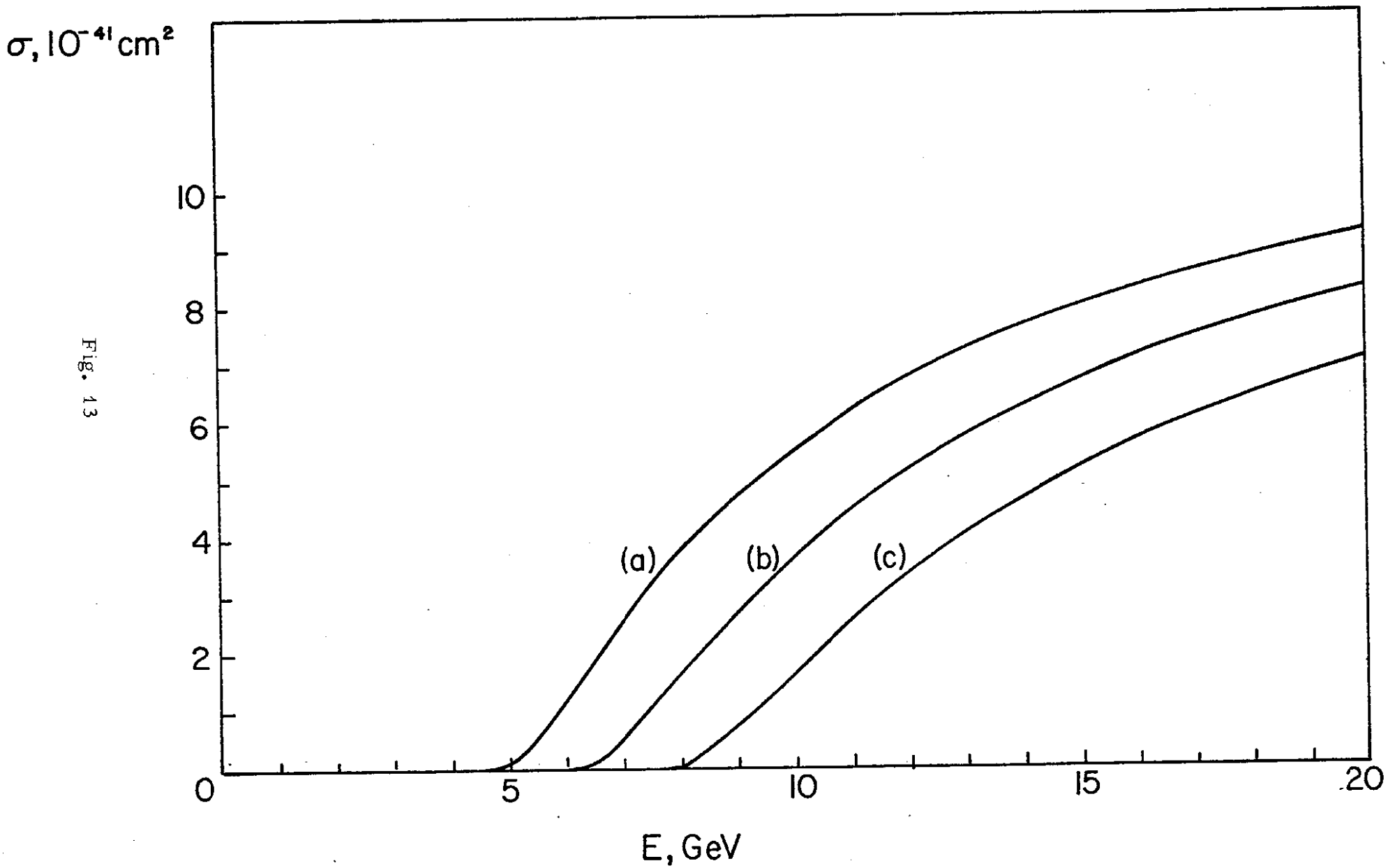

Fig. 13

$$20 \times 15 = 140 + 60^{*} + 36^{*} + 20' + (20)_1 + (20)_2 + 4^{*}$$

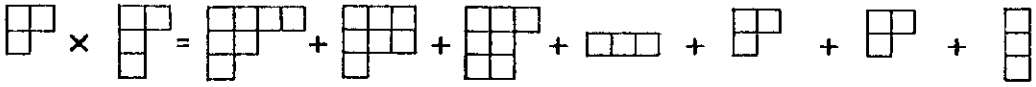

FIGURE 14